# SUPPORTING INFORMATION

## A supramolecular aggregate of four exchange-biased single-molecule magnets

Tu N. Nguyen[†], Wolfgang Wernsdorfer[‡], Khalil A. Abboud[†], George Christou[*,†]

*† Department of Chemistry, University of Florida, Gainesville, Florida, 32611-7200, USA,*

*‡ Institute Néel-CNRS 38042 Grenoble, Cedex 9, France*

***NMR spectra of pdpdH$_2$***

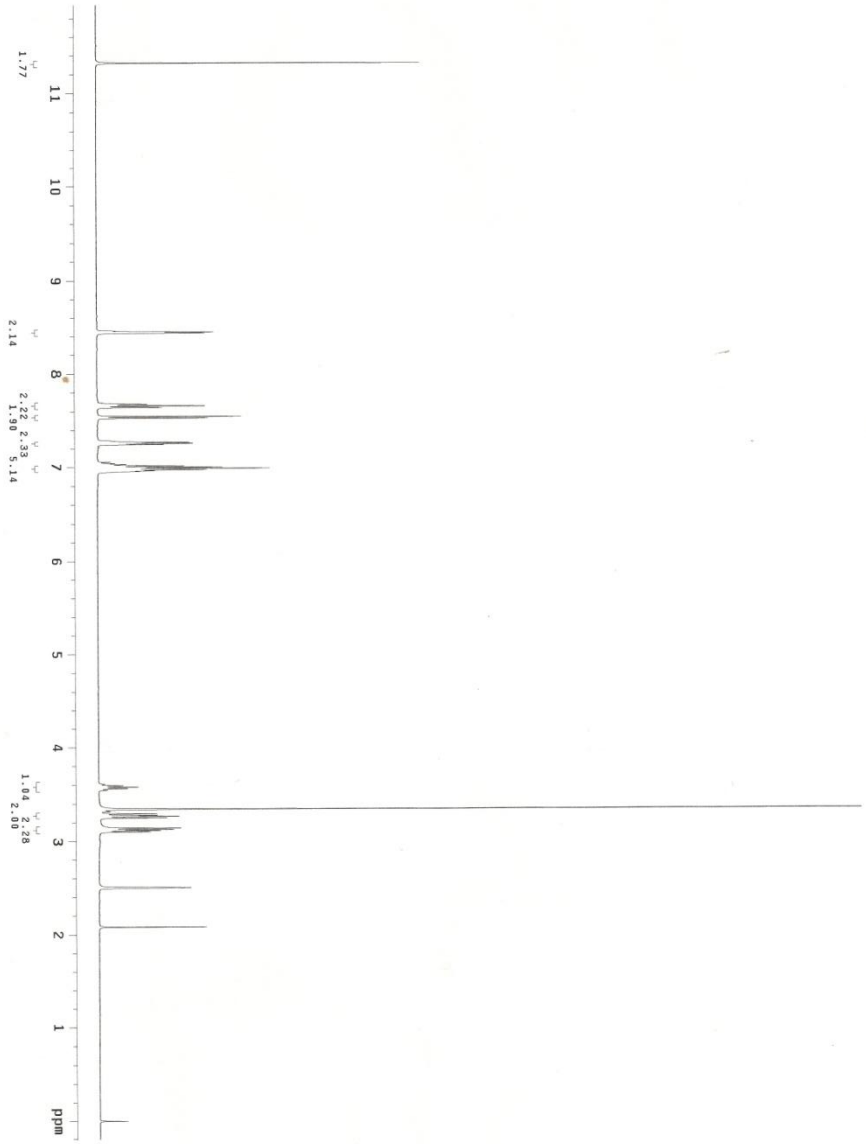



**Figure S1.** $^1$HNMR (DMSO, 500MHz) spectrum of pdpdH$_2$

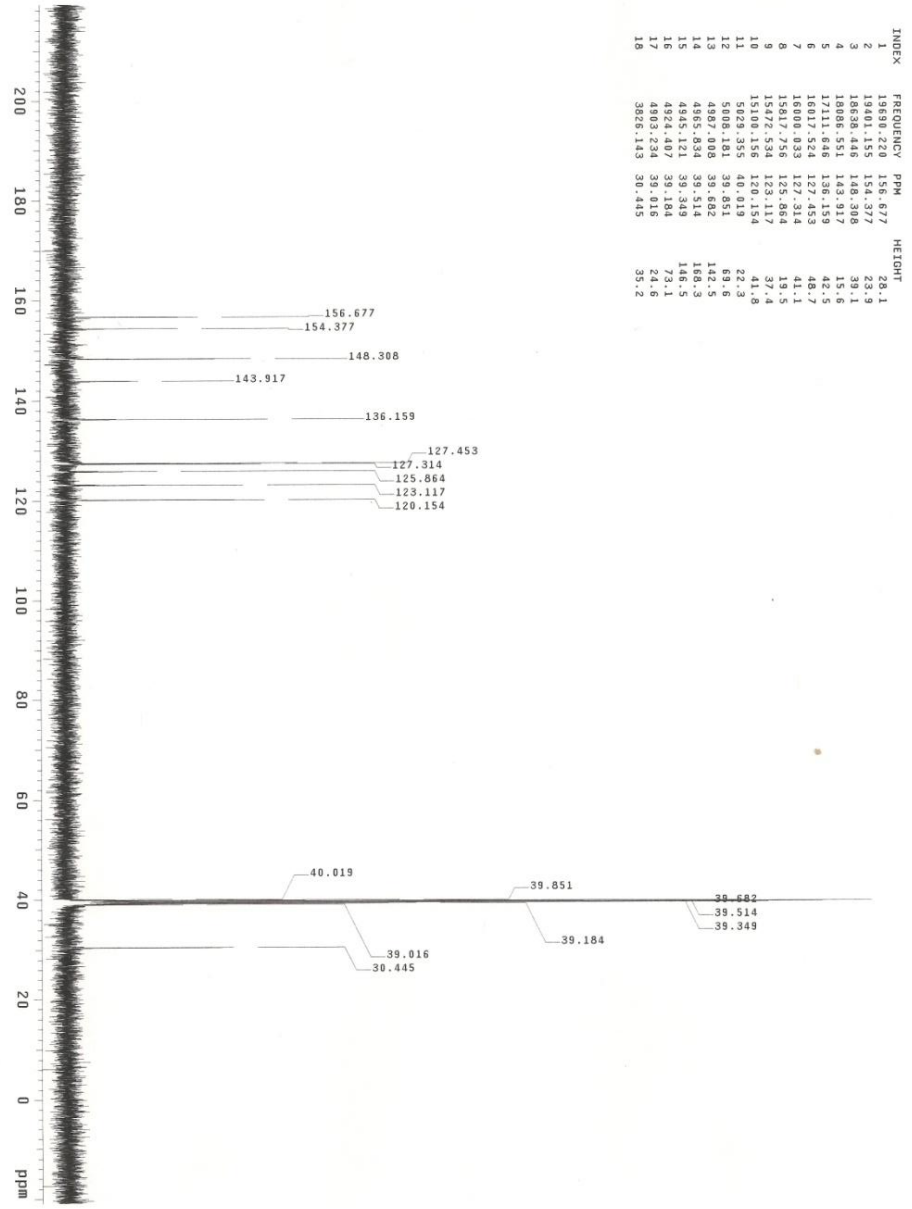



**Figure S2.** $^{13}$CNMR (DMSO, 500MHz) spectrum of pdpdH$_2$

$^{1}$H NMR (DMSO, 500 MHz): δ 11.32 (s, 2H, −OH), 8.44 (d, J = 4.81 Hz, 2H), 7.66 (t, J = 7.69 Hz, 2H), 7.54 (d, J = 7.82 Hz, 2H), 7.26 (t, J = 6.18 Hz, 2H), 6.99 (m, 5H), 3.58 (tt, J = 7.82 Hz, 7.82 Hz, 1H, −CH), 3.27 (dd, J = 12.42 Hz, 8.65 Hz, 2H, −$CH_2$), 3.12 (dd, J =12.42 Hz, 7.28 Hz, 2H, −$CH_2$).
$^{13}$C NMR (DMSO, 500 MHz): δ 156.7, 154.4, 148.3, 143.9, 136.2, 127.5, 127.3, 125.9, 123.1, 120.1, 30.4.

**CRYSTAL STRUCTURE**

There are approximately 52 $CH_2Cl_2$ molecules in the asymmetric unit (26 per $Mn_{12}$). Almost all are too disordered to be modeled, and the program SQUEEZE was used to calculate the solvent disorder area and remove its contribution to the overall intensity data.

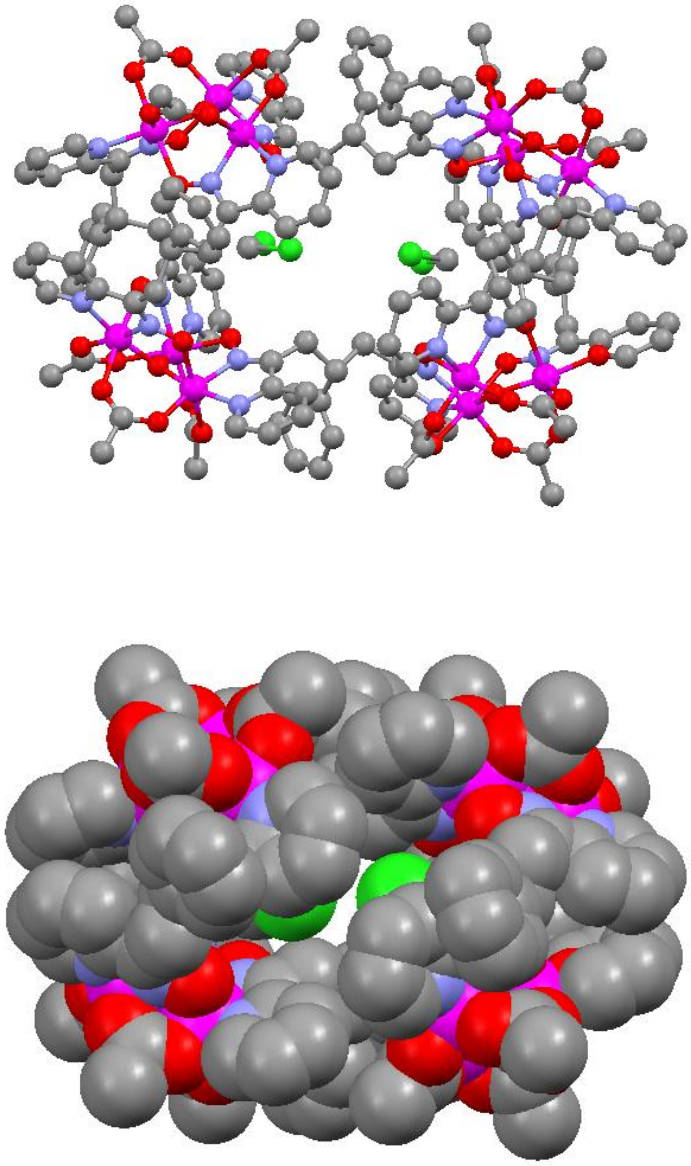


**Figure S3.** Encapsulation of two $CH_2Cl_2$ molecules inside the $Mn_{12}$ cation. H atoms have been removed for clarity.

**Table S1**. BVS calculations for the Mn[a] and selected O[b] atoms of complex **3**.

| | Mn(II) | Mn(III) | Mn(IV) | Assignment |
|---|---|---|---|---|
| Mn1 | 3.31 | **3.10** | 3.14 | Mn(III) |
| Mn2 | 3.26 | **3.04** | 3.09 | Mn(III) |
| Mn3 | 3.30 | **3.07** | 3.13 | Mn(III) |
| Mn4 | 3.35 | **3.13** | 3.17 | Mn(III) |
| Mn5 | 3.20 | **2.99** | 3.03 | Mn(III) |
| Mn6 | 3.31 | **3.10** | 3.14 | Mn(III) |
| Mn7 | 3.30 | **3.09** | 3.13 | Mn(III) |
| Mn8 | 3.37 | **3.12** | 3.16 | Mn(III) |
| Mn9 | 3.28 | **3.07** | 3.11 | Mn(III) |
| Mn10 | 3.28 | **3.07** | 3.11 | Mn(III) |
| Mn11 | 3.35 | **3.13** | 3.18 | Mn(III) |
| Mn12 | 3.43 | **3.22** | 3.25 | Mn(III) |
| Mn13 | 3.29 | **3.08** | 3.12 | Mn(III) |
| Mn14 | 3.30 | **3.09** | 3.13 | Mn(III) |
| Mn15 | 3.30 | **3.08** | 3.13 | Mn(III) |
| Mn16 | 3.30 | **3.08** | 3.13 | Mn(III) |
| Mn17 | 3.30 | **3.08** | 3.13 | Mn(III) |
| Mn18 | 3.24 | **3.03** | 3.07 | Mn(III) |
| Mn19 | 3.27 | **3.06** | 3.10 | Mn(III) |
| Mn20 | 3.28 | **3.07** | 3.11 | Mn(III) |
| Mn21 | 3.30 | **3.08** | 3.13 | Mn(III) |
| Mn22 | 3.25 | **3.04** | 3.08 | Mn(III) |
| Mn23 | 3.32 | **3.10** | 3.16 | Mn(III) |
| Mn24 | 3.25 | **3.04** | 3.08 | Mn(III) |

| | BVS | Assignment |
|---|---|---|
| O37 | **2.20** | $O^{2-}$ |
| O38 | **2.21** | $O^{2-}$ |
| O39 | **2.22** | $O^{2-}$ |
| O40 | **2.25** | $O^{2-}$ |
| O77 | **2.17** | $O^{2-}$ |
| O78 | **2.21** | $O^{2-}$ |
| O79 | **2.18** | $O^{2-}$ |
| O80 | **2.27** | $O^{2-}$ |

[a] The **bold** value is the one closest to the charge for which it was calculated. The oxidation state of a particular atom can be taken as the nearest integer to the value in bold.
[b] The O atom is not protonated if the BVS is ~1.8-2.2, mono-protonated if the BVS is ~1.0-1.2, and doubly-protonated if the BVS is ~0.2-0.4.

**Table S2.** Selected interatomic distances and angles for complex **3** for both $Mn_{12}$ cations in the asymmetric unit.

| | | | |
|---|---|---|---|
| Mn1-Mn2 | 3.212(2) | Mn2-O37-Mn1 | 118.3(2) |
| Mn1-Mn3 | 3.1842(19) | Mn3-O37-Mn1 | 115.3(3) |
| Mn2-Mn3 | 3.2012(19) | Mn2-O37-Mn3 | 118.6(3) |
| Mn4-Mn5 | 3.1887(18) | Mn4-O38-Mn5 | 116.5(3) |
| Mn4-Mn6 | 3.1726(18) | Mn6-O38-Mn4 | 116.9(3) |
| Mn5-Mn6 | 3.216(2) | Mn6-O38-Mn5 | 118.2(3) |
| Mn7-Mn8 | 3.180(2) | Mn8-O39-Mn7 | 116.3(3) |
| Mn7-Mn9 | 3.206(2) | Mn9-O39-Mn7 | 118.0(3) |
| Mn8-Mn9 | 3.205(2) | Mn9-O39-Mn8 | 118.7(3) |
| Mn10-Mn11 | 3.1850(18) | Mn11-O40-Mn10 | 118.5(3) |
| Mn10-Mn12 | 3.197(2) | Mn10-O40-Mn12 | 116.6(3) |
| Mn11-Mn12 | 3.218(2) | Mn11-O40-Mn12 | 119.3(3) |
| Mn13-Mn14 | 3.2046(19) | Mn14-O78-Mn13 | 117.6(3) |
| Mn13-Mn15 | 3.1887(17) | Mn15-O78-Mn13 | 116.8(3) |
| Mn14-Mn15 | 3.1995(17) | Mn15-O78-Mn14 | 118.1(3) |
| Mn16-Mn17 | 3.204(2) | Mn16-O77-Mn17 | 117.1(3) |
| Mn16-Mn18 | 3.194(2) | Mn16-O77-Mn18 | 117.3(3) |
| Mn17-Mn18 | 3.205(2) | Mn18-O77-Mn17 | 116.9(3) |
| Mn19-Mn20 | 3.187(2) | Mn19-O80-Mn20 | 117.2(3) |
| Mn19-Mn21 | 3.2008(19) | Mn19-O80-Mn21 | 118.8(3) |
| Mn20-Mn21 | 3.191(2) | Mn21-O80-Mn20 | 116.8(3) |
| Mn22-Mn23 | 3.2109(17) | Mn22-O79-Mn23 | 117.9(3) |
| Mn22-Mn24 | 3.1946(17) | Mn22-O79-Mn24 | 116.8(3) |
| Mn23-Mn24 | 3.2116(19) | Mn23-O79-Mn24 | 117.7(2) |

**Table S3.** Displacement (r) of $\mu_3$-oxide ions from $Mn_3$ planes, and the Mn-N-O-Mn torsion angles ($\theta$) in complex **3**.

| Triangle | r (Å) | Torsion Angles | θ (°) |
|---|---|---|---|
| Mn1Mn2Mn3 | 0.31 | Mn1-N19-O10-Mn3 | 17.98 |
| | | Mn2-N1-O1-Mn1 | 14.49 |
| | | Mn3-N21-O11-Mn2 | 10.90 |
| Mn4Mn5Mn6 | 0.32 | Mn4-N17-O9-Mn5 | 19.82 |
| | | Mn5-N15-O8-Mn6 | 10.75 |
| | | Mn6-N28-O12-Mn4 | 18.28 |
| Mn7Mn8Mn9 | 0.29 | Mn7-N13-O7-Mn8 | 15.88 |
| | | Mn8-N11-O6-Mn9 | 9.97 |
| | | Mn9-N9-O5-Mn7 | 15.73 |
| Mn10Mn11Mn12 | 0.26 | Mn10-N7-O4-Mn11 | 15.57 |
| | | Mn11-N3-O2-Mn12 | 8.09 |
| | | Mn12-N5-O3-Mn10 | 12.59 |

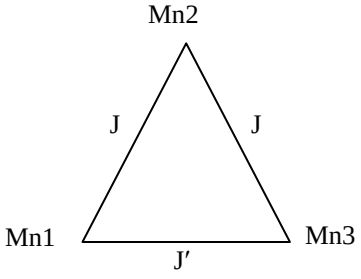
## FIT OF DC SUSCEPTIBILITY VS T DATA

The data were fit to the theoretical expression for four independent isosceles triangles, assuming that interactions between $Mn_3$ triangles are very weak compared to the interactions between Mn ions in each triangle.

**Fitting procedure:** $\chi_{[Mn3]4} = 4\chi_{Mn3} + TIP$

**Isosceles triangles (e.g. Mn1-Mn2-Mn3):**

$$\hat{S}_A = \hat{S}_1 + \hat{S}_3$$
$$\hat{S}_T = \hat{S}_A + \hat{S}_2$$
$$H = -2J(\hat{S}_1\hat{S}_2 + \hat{S}_2\hat{S}_3) - 2J'(\hat{S}_1\hat{S}_3)$$
$$H = -J(\hat{S}_T^2 - \hat{S}_A^2 - \hat{S}_2^2) - J'(\hat{S}_A^2 - \hat{S}_1^2 - \hat{S}_3^2)$$
$$E(S_T, S_A) = -J[S_T(S_T+1) - S_A(S_A+1)] - J'[S_A(S_A+1)]$$




**Isosceles triangle**

### VAN VLECK EQUATION

$\chi_{Mn3} = (Ng^2\mu_B^2/3kT)$**[** + 30.0000 *exp( 6.0000 *m+ 0.0000 *n)
+ 6.0000 *exp( 0.0000 *m+ 2.0000 *n)
+ 30.0000 *exp( 4.0000 *m+ 2.0000 *n)
+ 84.0000 *exp( 10.0000 *m+ 2.0000 *n)
+ 0.0000 *exp( -6.0000 *m+ 6.0000 *n)
+ 6.0000 *exp( -4.0000 *m+ 6.0000 *n)
+ 30.0000 *exp( 0.0000 *m+ 6.0000 *n)
+ 84.0000 *exp( 6.0000 *m+ 6.0000 *n)
+ 180.0000 *exp( 14.0000 *m+ 6.0000 *n)
+ 6.0000 *exp( -10.0000 *m+ 12.0000 *n)
+ 30.0000 *exp( -6.0000 *m+ 12.0000 *n)
+ 84.0000 *exp( 0.0000 *m+ 12.0000 *n)
+ 180.0000 *exp( 8.0000 *m+ 12.0000 *n)
+ 330.0000 *exp( 18.0000 *m+ 12.0000 *n)
+ 30.0000 *exp( -14.0000 *m+ 20.0000 *n)
+ 84.0000 *exp( -8.0000 *m+ 20.0000 *n)
+ 180.0000 *exp( 0.0000 *m+ 20.0000 *n)
+ 330.0000 *exp( 10.0000 *m+ 20.0000 *n)
+ 546.0000 *exp( 22.0000 *m+ 20.0000 *n)] /

[+ 5.0000 *exp( 6.0000 *m+ 0.0000 *n)
+ 3.0000 *exp( 0.0000 *m+ 2.0000 *n)
+ 5.0000 *exp( 4.0000 *m+ 2.0000 *n)
+ 7.0000 *exp( 10.0000 *m+ 2.0000 *n)
+ 1.0000 *exp( -6.0000 *m+ 6.0000 *n)
+ 3.0000 *exp( -4.0000 *m+ 6.0000 *n)
+ 5.0000 *exp( 0.0000 *m+ 6.0000 *n)
+ 7.0000 *exp( 6.0000 *m+ 6.0000 *n)
+ 9.0000 *exp( 14.0000 *m+ 6.0000 *n)
+ 3.0000 *exp( -10.0000 *m+ 12.0000 *n)
+ 5.0000 *exp( -6.0000 *m+ 12.0000 *n)
+ 7.0000 *exp( 0.0000 *m+ 12.0000 *n)
+ 9.0000 *exp( 8.0000 *m+ 12.0000 *n)
+ 11.0000 *exp( 18.0000 *m+ 12.0000 *n)
+ 5.0000 *exp( -14.0000 *m+ 20.0000 *n)
+ 7.0000 *exp( -8.0000 *m+ 20.0000 *n)

+ 9.0000 *exp( 0.0000 *m+ 20.0000 *n)
+ 11.0000 *exp( 10.0000 *m+ 20.0000 *n)
+ 13.0000 *exp( 22.0000 *m+ 20.0000 *n)]

where m = $J/kT$ and n = $J'/kT$

TIP = $6.0 \times 10^{-4}$

Constraints g > 1.85 and g<2.2

The fit gave:

J = 16.7771 ± 0.6111 $cm^{-1}$
J′ = 1.5439 ± 0.7360 $cm^{-1}$
g = 1.9140 ± 0.0029
R = 0.999, $R^2$ = 0.998

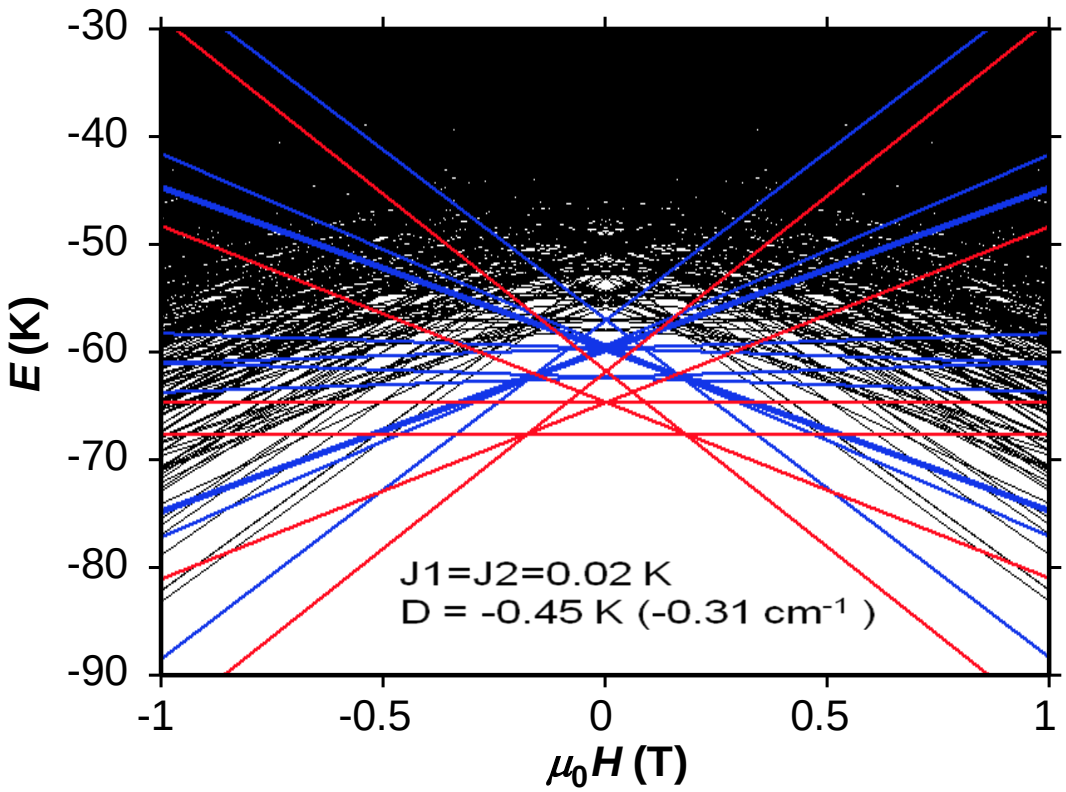



**Figure S4.** Simulation of the plot of spin state energies vs applied magnetic field for a tetramer of four $Mn_3$ SMMs, each with S = 6, that would give the avoided level crossings and QTM steps at the experimental values of ±0.18 T and 0 T for complex **3**. The simulation was with the $J_1$, $J_2$ and D values shown. Red = spin states involving only the $M_s$ = ±6 states of the four $Mn_3$ sub-units; Blue = spin states involving both $M_s$ = ±6 states and (only) one $M_s$ = ±5 state; Black = other states. See the text for the spin states involved in the three QTM steps in Fig. 6, which are all red levels.